INTRINSIC AND RESONANCE SPACE CHARGE LIMITS*

G. Parzen
Brookhaven National Laboratory
Upton, New York 11973

1. INTRODUCTION

The space charge limit in circular proton accelerators has been studied using a simulation program described below. Results from the simulation study indicate a different model for the space charge limit than the often presented models which emphasize reasonances due to magnetic field errors. This simulation study suggests that the intrinsic space charge limit plays an important role. The intrinsic space charge limit is the space charge limit, in the absence of magnetic field errors, and is due to the forces generated by the beam itself.

In studies of three operating accelerators, which include the AGS, the PS Booster, and the Fermilab booster, it was found that the computed intrinsic space charge limit was fairly close to the experimentally observed space charge limit. This result plus studies of the effects of resonances due to magnetic field errors suggest that the intrinsic space charge limit provides an upper bound for the space charge limit which is not far from what is actually achieved by operating accelerators.

The resonances present due to magnetic field errors, if strong enough, can prevent the accelerator from achieving the intrinsic space charge limit. However, the effects of these resonances were found to be appreciable only when the beam intensity gets close to the intrinsic space charge limit. Well below the intrinsic space charge limit, there is little beam growth due to magnetic field error driven resonances, and the space charge forces tend to stabilize these resonances.

The simulation program uses a tracking program, which tracks particles around the accelerator element by element. Space charge forces are entered as a kick at the entrance and exit of each element, and the kick is determined by the electric field E_x, E_y due to the beam, and the length of the element. To compute the electric field of the beam, the beam shape in x,y space is assumed to be gaussian with the two parameters σ_x, σ_y which are different at each element of the lattice. The parameters σ_x, σ_y are determined by tracking a sample of about 16 to 24 particles. The growth in the sample determines the growth in σ_x, σ_y.

The actual lattice of the accelerator is entered into the tracking program. This may be important in computing the intrinsic space charge limit.

2. INTRINSIC SPACE CHARGE LIMIT

The intrinsic space charge limit is the space charge limit in the absence of magnetic field errors. This limit is due to forces generated by the beam itself. The effect of the magnetic field errors, and the resonances generated by these errors, will be studied in Section 3.

2.1 Simulation Program for the Intrinsic Space Charge Limit

The accelerator is described as a series of elements. Each element may be a dipole, a quadrupole, or a sextupole or a field free drift space. Each element has a definite known transfer function and given the coordinates of a particle at the entrance to an element, one can compute the particle coordinates at the exit of the element using the transfer function. The motion of a particle over many turns can be studied by tracking the particles around the accelerator, element by element, over many turns. Using the actual lattice in studying the space charge limit, rather than some simple mathematical representation of the restoring force of the betatron oscillations, may be of importance in describing the effects of non-linear resonances which are derived by the beam forces.

The space charge forces are entered by giving the particle a kick, at the entrance and exit of each element, which is proportional to the electric field, E_x and E_y, produced by the beam and to the length of the element. To compute the electric field due to the beam, the beam shape in x,y space is assumed to be gaussian with two parameters σ_x, σ_y which are different at every element in the lattice. The parameters σ_x, σ_y are determined by tracking a sample of about 16 to 24 particles. The growth of the sample determines the growth in σ_x, σ_y.

It is assumed that the beam starts with a shape that is roughly gaussian in x,y space, and that as the beam grows, the beam shape remains roughly gaussian. It is assumed that the beam growth is not very sensitive to the beam shape, and that beams that are roughly gaussian will experience similar beam growths.

For a given N_B, the number of protons/bunch, the beam size will grow to a certain level and then stop growing. As N_B is increased, the final beam size gets larger. The value of N_B when the beam size reaches the vacuum chamber, is taken to be the space charge limit.

2.2 Intrinsic Space Charge Limit for the AGS

The simulation program described above was applied to compute the intrinsic space charge limit of the AGS accelerator at Brookhaven National Laboratory. The actual lattice of the AGS was used in the study.

Beam Growth

The growth of the beam as a function of N_B, the number of protons/bunch is shown in Fig. 2.2-1 for the case of a flat beam whose initial dimensions are ±21 × 11mm. The ±21mm is reached at a $\beta_{x,max}$ location, and the ±11mm at a $\beta_{y,max}$ location. The initial emittances of the beam are $\varepsilon_{BM,O}$ = 20,5mm • mrad corresponding to the initial beam size $X_{BM,O}$ = 21,11mm. In Fig. 2.2-1, XMX, YMX give the largest x and y reached by the beam. The aperture limits are also shown in Fig. 2.2-1 as X-Limit and Y-Limit. The value of N_B at which XMX, YMX reach one of the aperture limits is considered to be the space charge limit for this initial beam shape. For $\varepsilon_{BM,O}$ = 20,5 this happens when $N_B = .37 \times 10^{13}$/bunch.

AGS Space Charge Limit

The space charge limit depends on the initial beam shape. The space charge limit, $N_{B,L}$ as a function of the initial horizontal beam size $X_{BM,O}$ is shown in Fig. 2.2-2. The initial vertical beam size is held constant at $Y_{BM,O}$ = 11mm, $\varepsilon_{y,O}$ = 5mm•mrad. The largest space charge limit of $N_{B,L} = .37 \times 10^{13}$ is found for the initial beam size $X_{BM,O}$ = 21,11mm or $\varepsilon_{BM,O}$ = 20,5. The largest N_B achieved at the AGS, $N_B = .2 \times 10^{13}$, is shown by the dashed line and is about a factor of 2 below the maximum $N_{B,L}$.

2.3 Results for the AGS, the PS Booster and the Fermilab Booster

The simulation program was also applied to compute the intrinsic space charge limit of the PS Booster and the Fermilab Booster. The computed results for these two accelerators plus the computed results for the AGS can be compared with observations of the space charge limit[1,2,3] which is taken to be the highest intensity achieved by each of these accelerators.

The computed intrinsic space charge limit for these accelerators is shown in Fig. 2.3-1. For the AGS, the space charge limit is shown as a function of the initial maximum horizontal beam size, $X_{BM,O}$, the initial vertical size is held constant at a level corresponding to the initial vertical emittance $\varepsilon_{y,BM,O}$ = 5mm•mrad. For

---

*Work performed under the auspices of the U.S. Department of Energy

CH2669-0/89/0000-0818$01.00©1989 IEEE

the Fermilab booster the initial beam was assumed to be round with equal initial horizontal and vertical emittances $\varepsilon_{BM,o}$ and the space charge limit is shown as a function of $\varepsilon_{BM,o}$. For the PS booster the results shown are also for a round beam, and the results are not greatly different for a flat beam.

In Fig. 2.3-1 the approximate highest intensity reached at each of the 3 accelerators is shown by a dashed line. The maximum space charge limit found by the simulation program is about a factor of 2 larger than the highest intensity achieved for each of the 3 accelerators. In view of the approximations made in the program, this appears to be fairly good agreement between the results for the intrinsic limit and the experimentally measured limit. This suggests that the space charge limit may be largely determined by the intrinsic limit. This conjecture is further supported by studies presented in Section 3 of the effects of resonances driven by errors in the magnetic field.

2.4 Intrinsic Space Charge Limit for the AGS Booster

The simulation program was applied to compute the intrinsic space charge limit of the Booster for the AGS accelerator being built at Brookhaven National Laboratory.

Present plans are to achieve an intensity of $N_B = .5 \times 10^{13}$ protons/bunch which will lead to $N = 6 \times 10^{13}$ protons/pulse in the AGS.

AGS Booster Beam Growth

The growth of the beam as a function of N_B, the number of protons/bunch is shown in Fig. 2.4-1 for the case of a flat beam whose initial dimensions are ±22mm × ±8.5mm corresponding to initial emittances of $\varepsilon_{BM,O} = 33.5$mm • mrad. Of the 4 accelerators which were studied with the simulation program, the AGS Booster results were the most uncertain. The curve of YMX versus N_B, shown in Fig. 2.4-1, hovers near the Y-Limit over the range of $N_B = 1$ to $N_B = 3 \times 10^{13}$/bunch, where the curve is within a few mm of the Y-Limit. Thus, changes in the model used which change the Y growth by only a few mm can produce large changes in the space charge limit which is defined to be the value of N_B where YMX reaches the Y-Limit. For the case shown in Fig. 2.4-1, the intrinsic space charge limit is $N_B = 1.5 \times 10^{13}$ protons/bunch.

AGS Booster Intrinsic Space Charge Limit

The space charge limit, $N_{B,L}$, as a function of the initial horizontal beam size $X_{BM,O}$ is shown in Fig. 2.4-2. The initial vertical beam size is held constant at $Y_{BM,O}=8.5$mm, $\varepsilon_{y,o} = 5$mm•mrad. The largest space charge limit of $N_B = 1.5 \times 10^{13}$/bunch is found for the initial beam size $X_{BM,O} = 22$mm.

In Section 2.3 it was found that for three existing accelerators, the maximum computed intrinsic space charge limit was about a factor of 2 larger than the approximate highest intensity reached at these accelerators. Using this result, one can extrapolate from the maximum computed intrinsic space charge limit of $N_B = 1.5 \times 10^{13}$/bunch to find a space charge limit for the AGS Booster of $N_B = .75 \times 10^{13}$ protons/bunch.

3. THE EFFECTS OF RESONANCES DUE TO MAGNETIC FIELD ERRORS

The presence of random error fields in the magnets will drive linear and non-linear resonances. The ν-shift due to space charge forces can move the ν-values of some particles in the beam on to these resonances, causing the betatron oscillations of these particles to grow. The growth of the betatron oscillations is limited by the dependence of the ν-values on the amplitude of the betatron oscillations, which is also introduced by the space charge forces. Because of this limiting effect it is not clear that the resonance can seriously affect the space charge limit.[4] This section will discuss the results of a study using the simulation program of the effects of resonances on the space charge limit.

3.1 Procedure for Studying the Effects of Resonances

In order to drive the resonances, random error field multipoles a_k, b_k were introduced in each magnet of the lattice. The random error field in each magnet due to each multipole is given by

$$B_y=B_o b_k x^k \quad ,$$

$$B_x=B_o a_k x^k \quad ,$$

where B_o is the main dipole field. Studies were done for k = 1, random quadrupole errors, and for k = 2, random sextupole errors. The a_k and b_k are specified by their rms values, and each magnet has different a_k, b_k which are randomly chosen from a set of numbers with the given rms values.

In studying the effects of the random a_k, b_k, the beam is first allowed to grow due to space charge forces in the absence of random error field multipoles. When the beam reaches its final dimensions, the random a_k, b_k are then introduced and the particle motion is studied assuming that the beam dimensions are fixed. This procedure can be used to determine the onset of appreciable beam growth due to the random error a_k, b_k.

The above procedure appears safer than introducing the a_k, b_k at the very beginning and letting the beam grow due to space charge forces and the effects of the random a_k, b_k. The algorithm that has so far been used to compute the growth in the beam dimensions from the growth in the particles in the sample could be more in error in this situation. It is easier to understand and interpret the effects of random a_k, b_k when the beam dimensions are held fixed. The onset of appreciable growth due to the random a_k, b_k is often the result of interest. This allows us to set tolerances on the a_k, b_k to get little beam growth due to the random a_k, b_k.

The detailed results of this study of the effect of resonances will be given in another paper. The effects of resonances were found to be appreciable only when the beam intensity gets close to the intrinsic space charge limit. Well below the intrinsic space charge limit, there is little beam growth due to magnetic field error resonances, and the space charge forces tend to stabilize these resonances.

Acknowledgment

I wish to thank A.G. Ruggiero for several stimulating and helpful discussions. Thanks are also due to S.Y. Lee for AGS lattice data, to A.G. Ruggiero and S. Holmes for the Fermilab Booster lattice data and to W. Weng for the PS Booster lattice data. I wish to thank K. Jellett for considerable help with the programming and computer studies.

References

1. E. Raka, L. Ahrens, W. Frey, E. Gill, J.W. Glenn, R. Sanders and W. Weng, 1985 IEEE Particle Accel. Conf., p. 3110.
2. C. Ankenbrandt and S.P. Holmes, 1987 IEEE Particle Accel. Conf., p. 1066.
3. G. Gelato, L. Magnani, N. Ramussen, K. Schindl and H. Schonauer, 1987 IEEE Particle Accel. Conf. p. 1298.
   -J.P. Delahaye, G. Gelato, L. Magnani, G. Nassibian, F. Pedersen, K.H. Reich, K. Schindl and H. Schonauer, 11th International Conference on High Energy Accelerators, p. 299 (1980).
4. M. Month and W.T. Weng, 12th International Conference on High Energy Accelerators, 324 (1983).
   -W.T. Weng, Physics of Particle Accelerators, SLAC Summer School, 348 (1985).
   -I. Hofmann and K. Beckert, 1985 IEEE Particle Accelerator Conf., p. 2263.

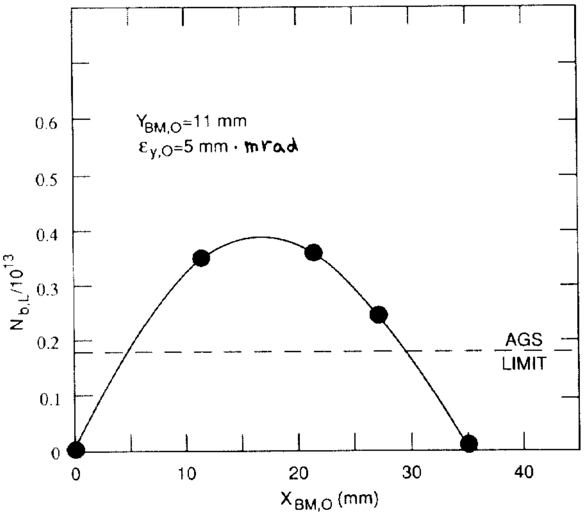

Fig. 2.2-2 AGS intrinsic space charge limit.

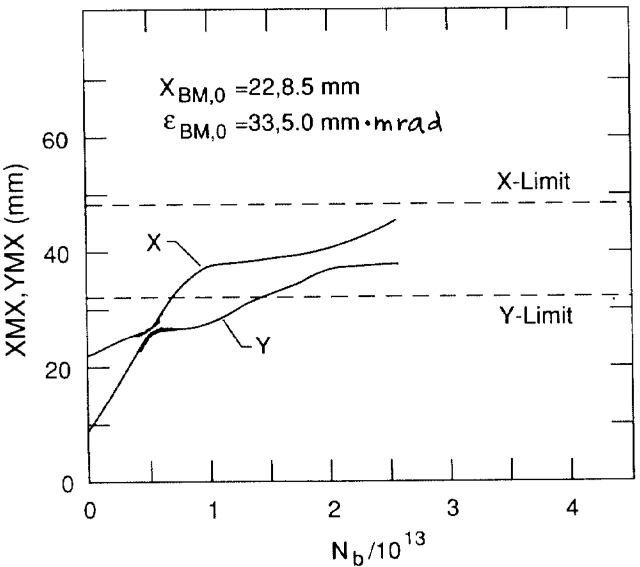

Fig. 2.4-1 AGS booster beam growth.

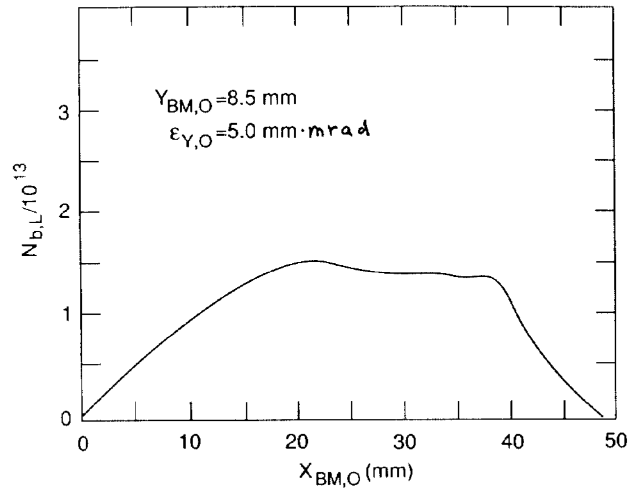

Fig. 2.4-2 AGS Booster intrinsic space charge limit.

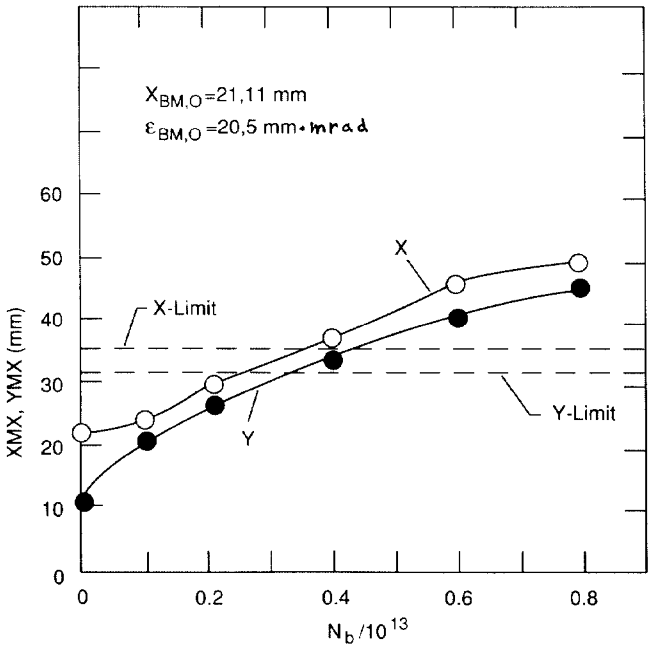

Fig. 2.2-1 AGS beam growth.

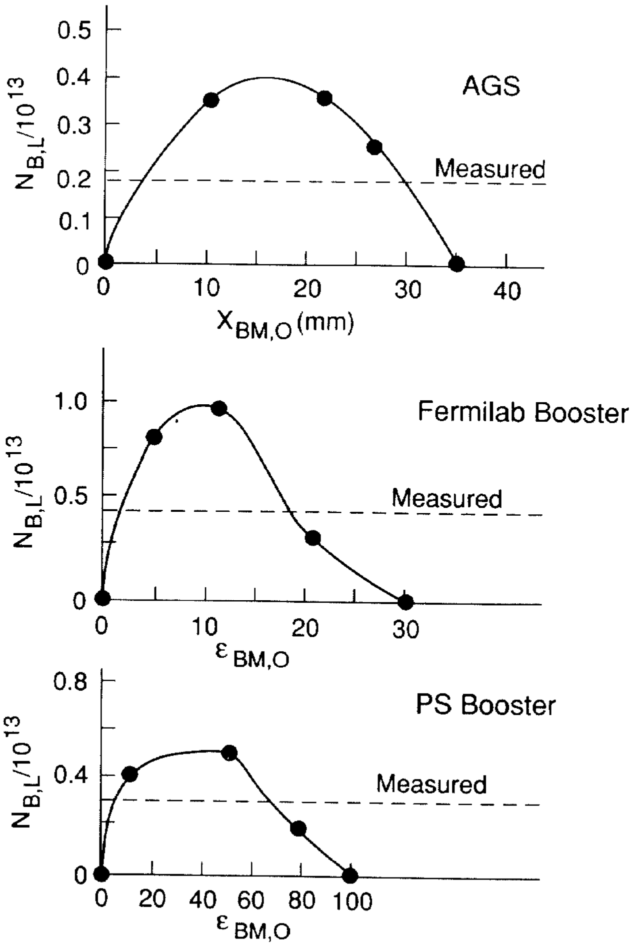

Fig. 2.3-1 Comparison of simulation programs results for the intrinsic space charge limit with measured results.